Bioorganic & Medicinal Chemistry 22 (2014) 6806–6813

Contents lists available at ScienceDirect

Bioorganic & Medicinal Chemistry

journal homepage: www.elsevier.com/locate/bmc

Synthesis of multi-galactose-conjugated 2′-*O*-methyl oligoribonucleotides and their in vivo imaging with positron emission tomography

Jussi Mäkilä [b], Satish Jadhav [a], Anu Kiviniemi [a], Meeri Käkelä [c], Heidi Liljenbäck [c,d], Päivi Poijärvi-Virta [a], Tiina Laitala-Leinonen [b], Harri Lönnberg [a], Anne Roivainen [c,d], Pasi Virta [a,*]

[a] Department of Chemistry, University of Turku, FI-20014 Turku, Finland
[b] Skeletal Biology Consortium, Department of Cell Biology and Anatomy, University of Turku, FI-20520 Turku, Finland
[c] Turku PET Centre, University of Turku and Turku University Hospital, FI-20520 Turku, Finland
[d] Turku Center for Disease Modelling, University of Turku, FI-20520 Turku, Finland

ARTICLE INFO

Article history:
Received 2 September 2014
Revised 22 October 2014
Accepted 24 October 2014
Available online 31 October 2014

Keywords:
Oligonucleotide-glyco-conjugates
^{68}Ga-labelled oligonucleotides
Solid-phase synthesis
PET-imaging
Liver targeting

ABSTRACT

^{68}Ga labelled 2′-*O*-methyl oligoribonucleotides (anti-miR-15b) bearing one, three or seven D-galactopyranoside residues have been prepared and their distribution in healthy rats has been studied by positron emission tomography (PET). To obtain the heptavalent conjugate, an appropriately protected 1,4,7-triazacyclononane-1,4,7-triacetic acid (NOTA) precursor bearing a 4-[4-(4,4′-dimethoxytrityloxy)butoxy]phenyl side arm was first immobilized via a base labile linker to the support and the oligonucleotide was assembled on the detritylated hydroxyl function of this handle. A phosphoramidite building block bearing two phthaloyl protected aminooxy groups and one protected hydroxyl function was introduced into the 5′-terminus. One acetylated galactopyranoside was coupled as a phosphoramidite to the hydroxyl function, the phthaloyl protections were removed on-support and two trivalent galactopyranoside clusters were attached as aldehydes by on-support oximation. A two-step cleavage with aqueous alkali and ammonia released the conjugate in a fully deprotected form, allowing radiolabelling with ^{68}Ga in solution. The mono- and tri-galactose conjugates were obtained in a closely related manner. In vivo imaging in rats with PET showed remarkable galactose-dependent liver targeting of the conjugates.

1. Introduction

Premature elimination via renal clearance, degradation by exonucleases, undesired accumulation in non-parenchymal cells of liver together with poor cellular uptake are hurdles of potential oligonucleotide-based drugs (antisense oligonucleotides and siRNA), which limit their systemic delivery to a target cell.[1–5] These shortcomings may at least partly be overcome by conjugation of oligonucleotides with agents exhibiting affinity to a certain cell-type.[6–9] Targeted delivery to a desired site of action may prevent waste accumulation, decrease passive time in the systemic circulation and enhance internalization by receptor-mediated endocytosis. Among the potential conjugate groups, sugars deserve a special attention, since their interaction with proteins (lectins) is responsible for many biologically important events such as cell–cell communication, host–pathogen interaction, immune response and cancer metastasis.[10–14] Affinity of monovalent carbohydrate ligand to proteins is generally low. Biologically relevant binding requires multiple simultaneous interactions of several identical sugars in a correct spatial arrangement.[15] To mimic these multivalent interactions, numerous artificial constructs have been prepared by decorating a variety of multiantennary scaffolds with monosaccharides.[16–19] Conjugation of such glycoclusters to therapeutic oligonucleotides may allow their targeting to lectin-like proteins present on the surface of certain cell types, and for this purpose, several approaches for the preparation of oligonucleotides bearing multiple sugar units have been described.[20–33] However, the data on the effects of carbohydrate conjugation on oligonucleotide distribution in vivo is still meagre. The early studies of Biessen et al.[34,35] have shown that a tetraantennary lysine-based galactose conjugate of a 20-mer ^{32}P-labeled oligodeoxyribonucleotide (ODN) is taken up in the liver of rat about four times as readily as its unconjugated counterpart. More recent studies with monovalent galactosylated polyethylene glycol conjugate of ^{33}P-ODN have indicated that hepatocytes rather than nonparenchymal cells were targeted.[36] Similarly, *N*-acetylgalactosylated (GalNAc)[37]

* Corresponding author. Tel.: +358 333 6777.
E-mail address: pamavi@utu.fi (P. Virta).

http://dx.doi.org/10.1016/j.bmc.2014.10.034
0968-0896/

and galactosylated[38] peptide nucleic acid (PNA) has been successfully targeted to rat liver. GalNAc-conjugated siRNAs which target transthyretin (TTR) mRNA have been shown to reduce TTR protein in blood in early stage human trials.[39] Very recent studies have verified that a triantennary GalNAc enhances the silencing potency of second-generation gapmer antisense oligonucleotides (ASOs) 6–10-fold in mouse liver.[40] To learn more about the role of the glyco-cluster effect on the whole body distribution of oligonucleotides, we now report on synthesis of mono-, tri- and hepta-valent galactose conjugates of a 2′-*O*-methyl oligoribonucleotide (anti-miR-15b) bearing a 3′-terminal (1,4,7-triazanonane-1,4,7-triyl)triacetic acid (NOTA) group and on positron emission tomography studies of the distribution of their ^{68}Ga complexes in healthy rats. An oligonucleotide conjugate without backbone modification was studied. The target miRNA (miR-15b) of the sequence is involved in hepatocyte apoptosis.[41,42]

2. Results and discussion

2.1. Synthesis of the PET-labelled oligonucleotide galactoconjugates (13–15)

Although several protocols for the preparation of oligonucleotide glycoconjugates are available,[20–33] incorporation of a metal-ion-binding functionality as an additional pendant group markedly complicates the synthesis. The most straightforward approach, viz. post synthetic conjugation with a bifunctional chelator[43] in solution, for example, suffers from insufficient difference in the chromatographic behavior between the radioligand-conjugate and the large parent oligonucleotide glycoconjugate.[44–48] To overcome this problem, a solid supported NOTA precursor was recently introduced.[49] The support allows automated assembly of 3′-radiometallated oligonucleotides, leaving the 5′-terminus free for further conjugation. In the present study, this support was applied for the preparation of 5′-glycoconjugated oligonucleotides. Figure 1 shows the structures of the non-nucleosidic phosphoramidite building blocks introduced to the 5′-terminus of the support bound oligonucleotides to allow subsequent galactose conjugation. Among these, 2-cyanoethyl 3-(4,4′-dimethoxytrityloxy)-2,2-bis{3-[(phthaliimidooxy)propyl]carbamoyl}propyl-*N*,*N*-diisopropylphosphoramidite (**1**)[50] and 2-cyanoethyl-5-(phthaliimidooxy)pent-1-yl-*N*,*N*-diisopropylphosphoramidite (**2**)[51] have been synthesized previously. 2-Cyanoethyl (methyl 2,3,4-tri-*O*-acetyl-α-D-galactopyranoside-6-*O*-yl)-*N*,*N*-diisopropylphosphoramidite (**3**) was obtained by phosphitylation of methyl 2,3,4-tri-*O*-acetyl-α-D-galactopyranoside[52] with 2-cyanoethyl *N*,*N*-diisopropylphosphoramidochloridite. The trivalent galactose cluster (**6**) was prepared according to a previously reported protocol[23] based on conjugation of 3-azidopropyl 2,3,4,6-tetra-*O*-acetyl-β-D-galactopyranoside (**4**)[53] to a 4-(tri-*O*-propargylpentaerythrityloxy)benzaldehyde (**5**)[22] scaffold by Cu(I) promoted click chemistry (Scheme 1). Esterified precursor of NOTA **7** was then immobilized to LCAA-CPG, as we have previously described (Scheme 2).[49] Pentane-1,5-diol was used instead of propane-1,3-diol for the transesterification step (step i in Scheme 2). This adjustment was noticed to improve the reproducibility of immobilization. On this support (**8**), a 22-mer 2′-*O*-methyl oligoribonucleotide (5′-UGU AAA CCA UGA UGU GCU GCU A-3′, anti-miR-15b) (**12**) was assembled on a 1.0 μmol scale on an automatic DNA/RNA-synthesizer. Non-nucleosidic phosphoramidites **1**–**3** were then coupled to the 5′-terminus, giving supports **9**–**11**. Benzylthiotetrazole as an activator and coupling times of 300 s and 600 s were used for the standard 2′-*O*-methyl ribonucleoside building blocks and for the non-nucleosidic phosphoramidites **1**–**3**, respectively. Support **9** was obtained by consecutive couplings of **1** and **3**. It should be noted that the branching unit (**1**) must be capped by a phosphodiester bond in order to stabilize the structure against base-catalyzed retro aldol condensation.[50] The phthaloyl protections of **9** and **10** were removed by a treatment with 0.5 mol L^{-1} hydrazinium acetate and then subjected to oximation with galactose cluster **6** (0.17 mol L^{-1} in MeCN, at rt for overnight).[23] In order to release the NOTA moiety as carboxylate, the solid supported conjugates were released using a previously optimized two step cleavage protocol[49]: first hydrolysis in aq NaOH (3 h at 55 °C) and then, after neutralization with NH_4Cl, conventional ammonolysis. The resulting conjugates **13**–**15** were purified by RP HPLC and their authenticity was verified by MS (ESI TOF) (cf. Table 1 and Fig. 5). Conjugate **16** was prepared earlier.[49] The isolated yields of conjugates **13** and **14** remained ca. 5% due to the known problems related to solid-supported oximation: that is, formation of formaldoximes (cf. the main side-product: t_r = 24 min with **13** in i/Fig. 5). Coupling of **3** did not show difference to standard nucleosidic phosphoramidite building blocks. The isolated yields (20%) of **15** and **16** were close to those obtained for 20-mer oligonucleotides in general.

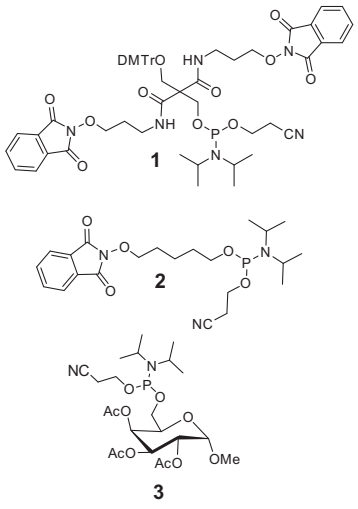

Figure 1. Non-nucleosidic phosphoramidite building blocks used for the synthesis of the conjugates **13**–**15**.

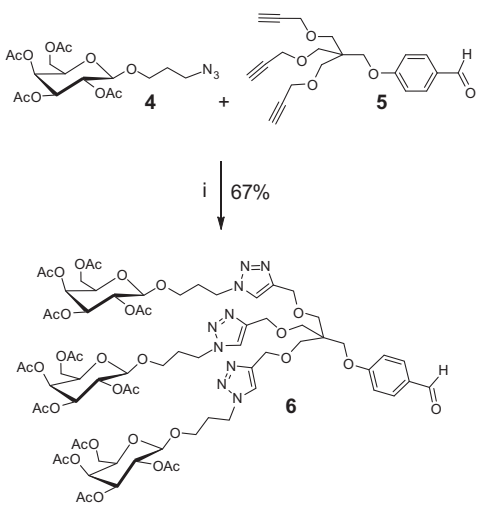

Scheme 1. Synthesis of the trivalent galactose cluster. Reagents: (i) $CuSO_4$, sodium ascorbate, H_2O, dioxane.

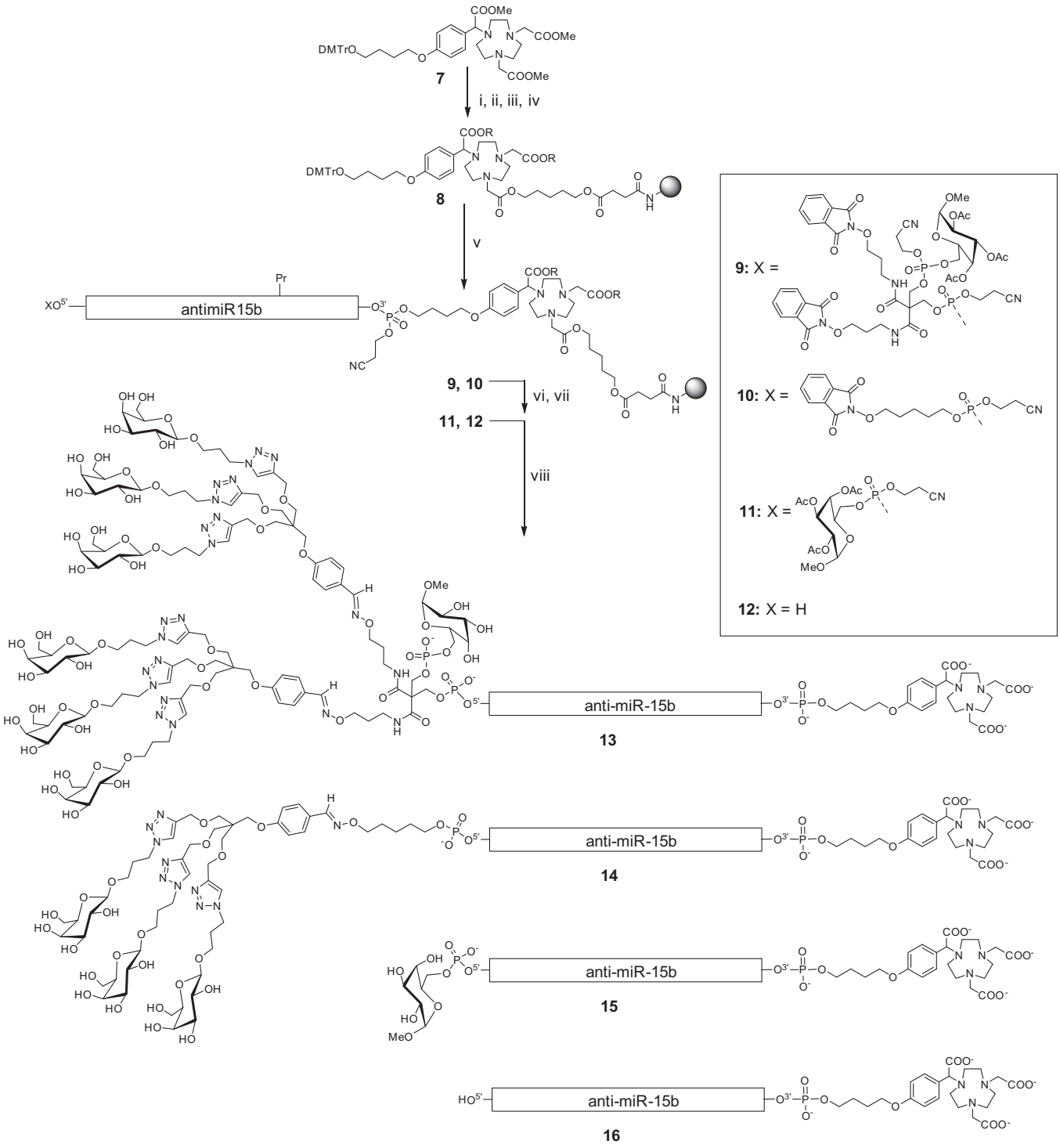

Scheme 2. Reagents and conditions: (i) $NaO(CH_2)_5OH$, in pentane-1,5-diol, MeCN, (ii) succinic anhydride, DMAP, pyridine, (iii) LCAA-CPG, PyBOP, DMAP, DMF, (iv) Ac_2O, 2,6-lutidine, *N*-methylimidazol, THF, (v) standard automated oligonucleotide synthesis by the phosphoramidite strategy, (vi) hydrazine acetate, AcOH, pyridine, (vii) 0.17 mol L^{-1} of **6** in MeCN, overnight at rt, (viii) (1) 0.1 mol L^{-1} aq NaOH, 3h at 55 °C (2) concd aq NH_3, overnight at 55 °C.

2.2. PET-imaging

Conjugates **13**–**16** were labelled as described earlier[44–46,49] and injected into the tail vein of Sprague–Dawley rats. The injection was followed by a 60 min dynamic PET-imaging with the high resolution research tomography. After imaging, the tissue samples of the euthanized animals were collected and the radioactivity concentrations were measured ex vivo with a gamma counter. Conjugates **13** (seven galactoses) and **14** (three galactoses) showed a high accumulation in liver (Fig. 2). In the ex vivo measurements, the liver radioactivity concentration of conjugate **13** was 8-fold higher compared to the nonglycosylated oligonucleotide **16** (P <0.05) and that of **14** 5-fold higher compared to **16** (Fig. 3). Conjugate **15** (one galactose) did not exhibit a significant difference in

Table 1
MS (ESI-TOF) data of the conjugates **13**–**15**

Entry	Oligonucleotide conjugate	Observed average molecular mass[a]	Calculated average molecular mass
1	**13**	10719.5	10719.0
2	**14**	9146.8	9148.6
3	**15**	8097.1	8097.4

[a] Calculated from the most intensive isotope combination at $[(M-11H+K)/10]^{-10}$.

the liver radioactivity compared to **16**. It may also be supposed that the seventh galactose unit of **13**, added mainly for synthetic reasons, is situated far from the six other galactose units and, hence, does not contribute to the recognition. According to the time-activity curves of the liver, **13** achieved a steady level of radioactivity at 6 min after intravenous injection (Fig. 4), while trivalent **14** experienced a slightly slower increase of radioactivity as a function of time after injection. The radioactivity level of the time-radioactivity curves of **15** and **16** was lower compared to **13** and **14**. Conjugate **16** showed the highest radioactivity, followed by **15**, both in the kidney ex vivo measurements (Fig. 3) and in the time–radio-activity curves (Fig. 4). The radioactivity of **13** and **14** was much lower in kidneys. Conjugate **13**, in turn, had the highest activity in urine according to both the ex vivo and the time–radioactivity data (Figs. 3 and 4). This appears paradoxal, because low kidney uptake should lead to low excretion into urine. This may be explained by metabolic cleavage of **13** that takes place in liver and release the PET tracer into urine. Recent studies of GalNac–ASO-conjugates have shown that only a small proportion of the conjugate could be extracted in intact form from liver even at 1 h timepoint.[40] It was also verified that metabolism occurred once the conjugate was internalized into the liver.

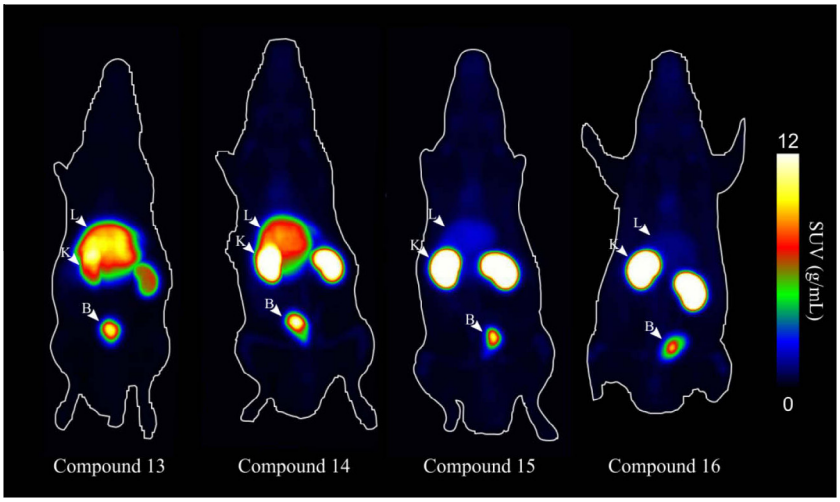

Figure 2. Maximum intensity projections of PET images. PET images are mean presentations of all time frames of 60-min acquisition. Liver (L) showed the highest radioactivity concentration with conjugate **13** (seven galactoses), kidneys (K) showed the highest radioactivity concentration with conjugate **16** (no galactose) and the highest radioactivity concentration in the urinary bladder (B) was observed with conjugate **13**.

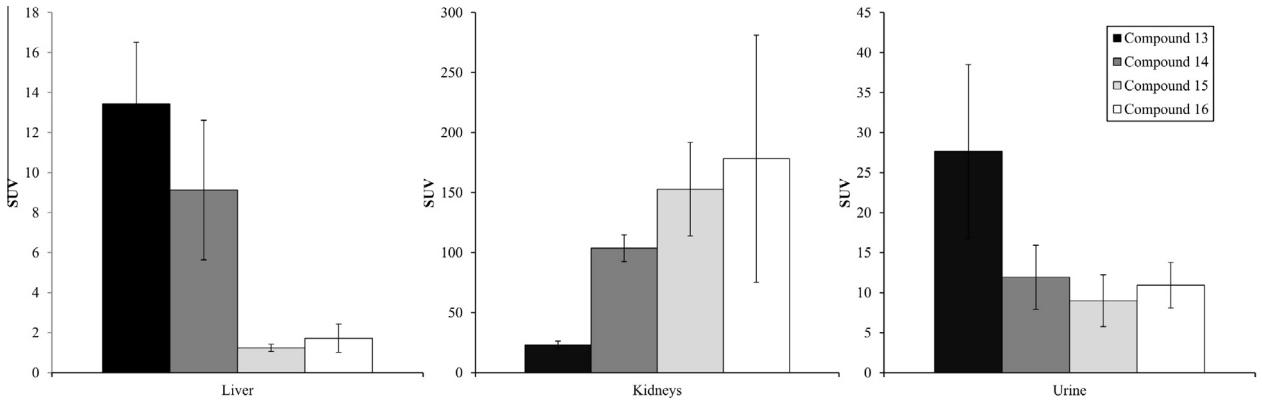

Figure 3. Ex vivo measured radioactivity concentration in rat liver, kidneys and urine samples.

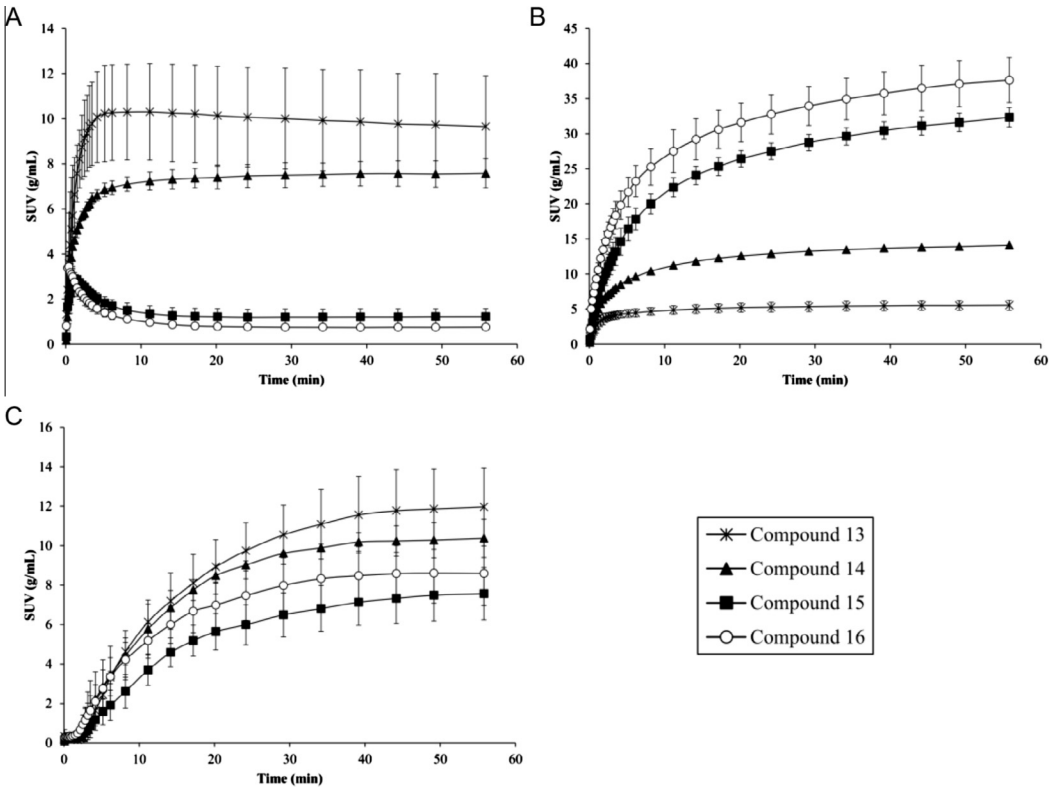

Figure 4. Time radioactivity curves of liver (A), kidneys (B) and urinary bladder (C).

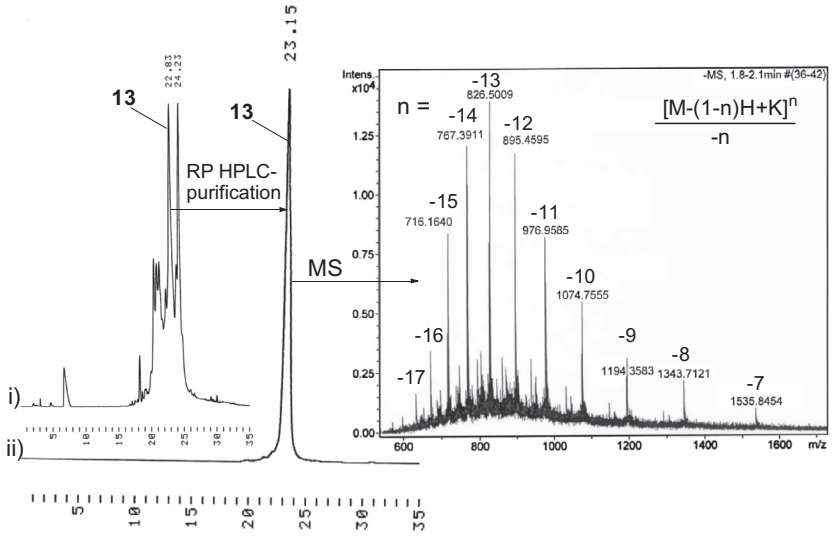

Figure 5. An example (the most complex conjugate **13**) of RP HPLC chromatograms (i: crude and ii: homogenized product) and MS (ESI-TOF) spectra of the conjugates. RP HPLC conditions: system B in General remarks.

3. Conclusions

^{68}Ga-labelled oligonucleotides (anti-miR-15b) bearing multiple galactose units on the 5′-terminus were synthesized using automated phosphoramidite chemistry and on-support oximation. A solid-supported NOTA precursor was applied for the synthesis, which, in contrast to post-synthetic labelling methods, gave the desired products without contamination by traces of unreacted radioligands. Whole-body biodistribution of the conjugates (**13**–**16**) in rats was monitored by PET. Among the compounds studies, the hepta-valent galactose conjugate (**13**) exhibited the highest and fastest uptake in liver, followed by the trivalent conjugate (**14**). Accordingly, the liver uptake correlated with the number of sugar residues on the conjugate. The liver-seeking conjugate **13** had the lowest kidney uptake among the oligonucleotide conjugates studied, but at the same time its excretion into urine was the highest.

Asialoglycoprotein receptor (ASGPR), abundantly expressed by mammalian liver parenchymal cells, recognizes galactose clusters on the surface of the glycoproteins and is important for the

endocytosis of these proteins.[41] The marked difference between the liver uptake of these conjugates (**13** > **14** ≫ **15** ~ **16**) may possibly be attributed to the glycocluster effect that takes place in binding to ASGP-R. It has been shown that ASGP-R usually clearly prefers trivalent glycoconstructs over their di- or monovalent counterparts.[54]

Kidney uptake of compound **13** was the lowest among the compounds studied. The increasing number of galactose ligands clearly reduced accumulation in kidneys. One reasonable explanation is the competition between the liver and kidneys, that is, excretion through hepatobiliar or renal pathways. However, compound **13** showed the highest radioactivity in urine (Fig. 4). This could be explained by the same behavior that has recently been observed with GalNac–ASO-conjugates:[40] that is, metabolic cleavage of the conjugate **13** in liver that release the PET-tracer into urine.

4. Experimental procedures

4.1. General remarks

The NMR spectra were recorded at 500 MHz. The chemical shifts are given in ppm from internal TMS. The mass spectra were recorded using a MS (ESI-TOF) spectrometer. RP HPLC analysis and purification of the oligonucleotides were performed using a Thermo ODS Hypersil C18 (150 × 4.6 mm, 5 μm) analytical column and a Phenomenex Oligo-RP C18 (250 × 10 mm, 5 μm) semi-preparative column with a gradient elution either (A) from 0% to 35% MeCN in aqueous 0.1 mol L^{-1} $Et_3NH^+AcO^-$ or (B) from 0% to 35% MeCN in aqueous 50 mmol L^{-1} $NH_4^+AcO^-$ (0–35 min). The flow rate was 1.0 mL min^{-1} (analytical) or 3.0 mL min^{-1} (semi-preparative) and the detection wavelength 260 nm. ^{68}Ga was obtained in the form of [^{68}Ga]Cl_3 from a ^{68}Ge/^{68}Ga generator (Eckert & Ziegler, Valencia, California, USA).

4.2. 2-Cyanoethyl (methyl 2,3,4-tri-*O*-acetyl-α-D-galacto-pyranoside-6-O-yl)-*N*,*N*-diisopropyl phosphoramidite (3)

Triethylamine (1.32 mL, 9.5 mmol) and 2-cyanoethyl *N*,*N*-diisopropylphosphoramidochloridite (500 μL, 2.3 mmol) were added to a mixture of methyl 2,3,4-tri-*O*-acetyl-α-D-galactopyranoside[52] (0.60 g, 1.9 mmol) in dichloromethane (7 mL) under nitrogen. After 2 h, the mixture was filtered through a short dried silica gel column (50% EtOAc in hexane, 0.1% Et_3N) to yield a mixture of R_P- and S_P-diastereomers of **3** (0.69 g, 70%) as colorless oil. ^{1}H NMR (500 MHz, CD_3CN a mixture of R_P and S_P diastereomers): δ 5.47–5.43 (m, 1H), 5.27 (dd, 1H, *J* = 10.8 and 3.3 Hz), 5.08 (dd, 1H, *J* = 10.5 and 3.5 Hz), 4.95 (d, 0.5H, *J* = 3.5 Hz), 4.95 (d, 0.5H, *J* = 3.5 Hz), 4.20–4.15 (m, 1H), 3.88–3.70 (m, 2.5H), 3.67 (dd, 1H, *J* = 7.5 and 7.0 Hz), 3.65–3.56 (m, 2.5H), 3.40 (s, 1.5H), 3.40 (s, 1.5H), 2.69–2.64 (m, 2H), 2.13 (s, 1.5H), 2.12 (s, 1.5H), 2.04 (s, 3H), 1.95 (s, 3H), 1.21–1.15 (m, 12H); ^{13}C NMR (125 MHz, CD_3CN): δ 170.2, 170.13, 170.13, 170.08, 169.87, 169.85, 68.2, 68.1, 67.9, 67.9, 67.8 (d, *J* = 7.1 Hz), 67.7 (d, *J* = 7.1 Hz), 67.54, 67.50, 61.2 (d, *J* = 17.0 Hz), 61.1 (d, *J* = 16.9 Hz), 58.5 (d, *J* = 18.6 Hz), 58.4 (d, *J* = 18.6 Hz), 54.85, 54.83, 42.9 (d, *J* = 5.6 Hz), 42.8 (d, *J* = 5.5 Hz), 23.95, 23.92, 23.90, 23.87, 20.1, 20.0, 19.94, 19.89; ^{31}P NMR (200 MHz, CD_3CN): δ 148.64 and 148.56; HRMS (ESI): $[M+H]^+$ $C_{22}H_{38}N_2O_{10}P$ requires 521,2264, found 521.2281.

4.3. Trivalent galactose cluster (6)

3-Azidopropyl 2,3,4,6-tetra-*O*-acetyl-β-D-galactopyranoside (**4**)[53] (64 mg, 0.18 mmol) and 4-[3-(prop-2-yn-1-yloxy)-2,2-bis(prop-2-yn-1-yloxymethyl)propoxy]benzaldehyde (**5**)[23] (370 mg, 0.86 mmol) were dissolved in 1,4-dioxane (1.3 mL) and the aqueous solutions of $CuSO_4{\cdot}5H_2O$ (36 μL, 50 mmol L^{-1}) and sodium ascorbate (900 μL, 0.1 mol L^{-1}) were added. The mixture was first heated at 50 °C for 4 h, and then stirred at room temperature overnight. To complete the reaction, an additional heating at 50 °C for 5 h was required. The reaction mixture was evaporated to dryness and the residue was dissolved in EtOAc and washed twice with brine. The organic fraction was dried with Na_2SO_4, evaporated to dryness and purified by silica gel chromatography (5% MeOH in EtOAc). Cluster **6** (0.20 g) was obtained as white foam in 67% yield. ^{1}H NMR (500 MHz, $CDCl_3$): δ_{ppm} 9.89 (s, 1H), 7.82 (d, 2H, *J* = 8.7 Hz), 7.51 (s, 3H), 6.96 (d, 2H, *J* = 8.7 Hz), 5.40 (br d, 3H, *J* = 3.2 Hz), 5.21 (dd, 3H, *J* = 10.4 and 8.0 Hz), 5.03 (dd, 3H, *J* = 10.5 and 3.4 Hz), 4.58 (s, 6H), 4.48 (d, 3H, *J* = 8.0 Hz), 4.44 (m, 3H), 4.35 (m, 3H), 4.19–4.09 (m, 6H), 4.03 (s, 2H), 3.94–3.87 (m, 6H), 3.61 (s, 6H), 3.49 (m, 3H), 2.21–2.08 (m, 6H), 2.16 (s, 9H), 2.09 (s, 9H), 2.04 (s, 9H), 1.99 (s, 9H); ^{13}C NMR (125 MHz, $CDCl_3$): δ_{ppm} 190.7, 170.3, 170.2, 170.1, 169.6, 164.1, 145.0, 131.9, 130.0, 122.7, 114.8, 101.2, 70.8, 70.7, 68.8, 68.7, 67.0, 66.0, 64.9, 61.2, 46.7, 45.1, 30.3, 20.9, 20.7, 20.7, 20.6; HRMS (ESI): $[M+Na]^+$ $C_{72}H_{97}N_9NaO_{35}$ requires 1670.5985, found 1670.5993.

4.4. NOTA-CPG-support (8)

Dimethyl [7-(1-{4-[4-(4,4′-dimethoxytrityloxy)butoxy]phenyl}-2-methoxy-2-oxoethyl)-1,4,7-triazacyclononane-1,4-diyl]diacetate (**7**, 30 mg, 37 μmol) was synthesized as previously described[49] and dissolved in a mixture of 0.1 mol L^{-1} $NaO(CH_2)_5OH$ in 1,5-pentanediol (0.2 mL) and MeCN (1.8 mL) (step i in Scheme 2). The mixture was stirred for 3 h at ambient temperature, neutralized by addition of pyridinium hydrochloride (60 mg), diluted with DCM and washed with saturated $NaHCO_3$ and brine. The organic layer was dried with Na_2SO_4, filtered and evaporated to dryness. The residue, succinic anhydride (4.0 mg, 39 μmol) and a catalytic amount of 4-(*N*,*N*′-dimethylamino)pyridine (DMAP) were dissolved in dry pyridine (0.5 mL), the mixture was stirred overnight at ambient temperature and evaporated to dryness (step ii in Scheme 2). The residue was dissolved in dry DMF (1.5 mL), suspended with long chain alkylamine controlled pore glass (LCAA-CPG)-support (350 mg), PyBOP (38 mg, 73 μmol), DMAP (4.0 mg, 32 μmol) and DIEA (26 μL) were added, and the suspension was shaken overnight at ambient temperature (step iii in Scheme 2). The crude NOTA-loaded support **8** was filtered, washed with DMF, DCM and MeOH, and dried under vacuum. The unreacted hydroxyl groups and amino groups on the parent support were finally capped by acetylation: The support was suspended in a mixture of Ac_2O, 2,6-lutidine and *N*-methylimidazol in THF (5:5:8:82, v/v/v/v, for 2 × 15 min at 25 °C), washed with DMF, DCM and MeOH and dried under vacuum. According to DMTr-cation assay, a loading of 27 μmol g^{-1} was obtained. An automatic test synthesis with a short oligonucleotide (T_6), followed by cleavage and RP HPLC and MS (ESI-TOF) analysis of the product, verified the quality of support **8**.

4.5. Synthesis of oligonucleotide conjugates 13–16

The 22-mer 2′-*O*-methyl oligoribonucleotide (anti-miR-15b) was assembled on an automatic DNA/RNA-synthesizer on four parallel batches (each in 1.0 μmol scale) of support **8**.[49] Standard RNA coupling cycle (300 s coupling time using benzylthiotetrazole as an activator) was used. For the synthesis of the galactose conjugates (**13**–**15**), phthalimidooxy- (**1** and **2**)[50,51] and galactose-derived (**3**) phosphoramidites were introduced to the 5′-terminus of the supported oligonucleotides (**9**–**11** in Scheme 2). A prolonged 600 s coupling time and slightly elevated phosphoramidite concentration (0.13 mol L^{-1} solution of **1**, **2** or **3** in MeCN used to load the reagent vessel) gave quantitative couplings for these non-nucleosidic building blocks. The support obtained by coupling branching

unit **1** was subjected to an additional detritylation step[50] and subsequent coupling of **3**. After the chain assembly, supports **9** and **10** were removed from the synthesizer, treated in reaction columns with a mixture of 0.5 mol L^{-1} hydrazinium acetate in AcOH–pyridine (1:4, v/v, 15 min at rt), washed with pyridine and MeCN and dried under vacuum. Triantennary galactose cluster **6** was then conjugated to the exposed aminooxy groups by on-support oximation.[50,51] The supports were transferred to microcentrifuge tubes and suspended in a 0.17 mol L^{-1} solution of **6** in dry MeCN.[23] The suspensions were shaken overnight at ambient temperature, filtered, washed with MeCN, and dried under vacuum. Finally, the oligonucleotide conjugates were released from the support and deprotected by previously optimized two-step cleavage protocol[49]: (step 1/viii in Scheme 2) The supports in microcentrifuge tubes were treated with 0.1 mol L^{-1} aq NaOH (1.0 mL) for 3 h at 55 °C. The suspensions were neutralized by addition of 1.0 mol L^{-1} aqueous ammonium chloride (1.1 mL), filtered and the filtrates were evaporated to dryness (step 2/viii in Scheme 2). The residues were dissolved in concentrated aqueous ammonia (overnight at 55 °C) and evaporated to dryness. The crude products **13–16** were purified by RP HPLC and their authenticity was verified by MS (ESI-TOF) (See Table 1 and Fig. 5, characterization data for **16**, see Ref. 49).

4.6. ^{68}Ga labelling of conjugates 13–16.

^{68}Ga was obtained in the form of $[^{68}Ga]Cl_3$ from a $^{68}Ge/^{68}Ga$ generator (instrument details in general remarks) by elution with 0.1 mol L^{-1} HCl. Sodium acetate was then added to give a 0.4 mol L^{-1} solution with regard to sodium acetate. The pH was adjusted to 3.5 with HCl, an oligonucleotide conjugate (**13–16**, 5–12 nmol, as a 1 mM solution) was added and the reaction mixture was incubated at 95 °C for 10–15 min. The radiochemical purity of [^{68}Ga]-chelated **13–16** was determined by a RP radio-HPLC (see instrument details in general remarks) with a gradient elutions either from 0.1 mol L^{-1} $Et_3NH^+AcO^-$ in H_2O to 0.1 mol L^{-1} $Et_3NH^+AcO^-$ in 50% aq MeCN or from 50 mmol L^{-1} $NH_4^+AcO^-$ in H_2O to 50 mmol L^{-1} $NH_4^+AcO^-$ in 50% aq MeCN. After each run, the column was washed with 50 mmol L^{-1} aqueous phosphoric acid.

4.7. Dynamic PET-imaging of the biodistribution

Fourteen male and two female Sprague–Dawley rats were used (n = 2–6 per tracer; weight 358 ± 70 g) in the study. Labelled tracers (17.3 ± 5.8 MBq per animal, specific radioactivity 5.08 ± 0.35 MBq/nmol) were injected into the tail vein. The injection was followed by a 60 min dynamic PET-imaging with the High Resolution Research Tomography (Siemens Medical Solutions, Knoxville, TN, USA). Two rats were imaged simultaneously. For PET imaging, rats were anesthetized with isoflurane and placed on a thermal pad. After the scan the collected imaging data was reconstructed with the ordered-subsets expectation maximization 3D algorithm (OSEM3D). Quantitative analysis was performed by defining volumes of interest (VOI) on the liver, kidneys and urinary bladder areas (Carimas 2.8; Turku PET Centre, Turku, Finland; http://www.turkupetcentre.fi/carimas). The average radioactivity concentration in the VOI (kBq/mL) was used for further analyses. The uptake was reported as a standardized uptake value (SUV), which was calculated as a ratio of radioactivity of the VOI and injected radioactivity (kBq) divided by body weight (g). Time–radioactivity curves, representing radioactivity concentration in the organ of interest versus time after tracer injection, were extracted from dynamic images accordingly. After imaging, the animals were euthanized and tissue samples were collected, weighed and radioactivity concentrations were measured ex vivo with the 1480 Wizard 3″ gamma counter (Perkin Elmer, Turku, Finland). The radioactivity uptake was reported as SUV. All animal experiments were approved by the national Animal Experiment Board in Finland and carried out in compliance with the European Union laws relating to the conduct of animal experimentation.

Acknowledgments

The financial support from the Academy of Finland (251539, 252097, 256214 and 258814) and from the Erasmus Mundus Action 2, Strand 1 (EMA2) for the award of EXPERTS fellowships are gratefully acknowledged.

Supplementary data

Supplementary data (additional material for the preparation of **3**, NMR spectra (^{1}H, ^{13}C, ^{31}P, COSY and HSQC) of **3** and **6** and table considering ex vivo-biodistribution of intravenously injected ^{68}Ga labeled compounds **13–16** in healthy rats) associated with this article can be found, in the online version, at http://dx.doi.org/10.1016/j.bmc.2014.10.034.

References and notes

1. Burnett, J. S.; Rossi, J. J. *Chem. Biol.* **2012**, *19*, 60.
2. Kole, R.; Krainer, A. R.; Altman, S. *Nat. Rev. Drug Discovery* **2012**, *11*, 125.
3. Juliano, R. L.; Ming, X.; Nakagawa, O. *Bioconjugate Chem.* **2012**, *23*, 147.
4. Kurreck, J. *Angew. Chem., Int. Ed.* **2009**, *48*, 1378.
5. Castanotto, D.; Rossi, J. J. *Nature* **2009**, *457*, 426.
6. Juliano, R. L.; Ming, X.; Carver, K.; Laing, B. *Nucleic Acid Ther.* **2014**, *24*, 101.
7. Winkler, J. *Ther. Delivery* **2013**, *4*, 791.
8. Ming, X. *Exp. Opin. Drug Delivery* **2011**, *8*, 435.
9. Marlin, F.; Simon, P.; Saison-Behmoares, T.; Giovannangeli, C. *ChemBioChem* **2010**, *11*, 1493.
10. Ernst, B.; Magnani, J. L. *Nat. Rev. Drug Discovery* **2009**, *8*, 661.
11. Seeberger, P. H.; Werz, D. B. *Nature* **2007**, *446*, 1046.
12. Collins, B. E.; Paulson, J. C. *Curr. Opin. Chem. Biol.* **2004**, *8*, 617.
13. Bertozzi, C. R.; Kiessling, L. L. *Science* **2001**, *291*, 2357.
14. Lis, H.; Sharon, N. *Chem. Rev.* **1998**, *98*, 637.
15. Dam, T. K.; Brewer, C. F. *Adv. Carbohydr. Chem. Biochem.* **2010**, *63*, 139.
16. Blanco, J. L. J.; Mellet, C. O.; Fernández, J. M. G. *Chem. Soc. Rev.* **2013**, *42*, 4518.
17. Wittmann, V.; Pieters, R. J. *Chem. Soc. Rev.* **2013**, *42*, 4492.
18. Chabre, Y. M.; Roy, R. *Chem. Soc. Rev.* **2013**, *42*, 4657.
19. Lee, R. T.; Wang, M.-H.; Lin, W.-J.; Lee, Y. C. *Bioorg. Med. Chem.* **2011**, *19*, 2494.
20. Aviñó, A.; Ocampo, S. M.; Lucas, R.; Reina, J. J.; Morales, J. C.; Perales, J. C.; Eritja, R. *Mol. Divers.* **2011**, *15*, 751.
21. Kiviniemi, A.; Virta, P.; Lönnberg, H. *Bioconjugate Chem.* **2011**, *22*, 1249.
22. Ugarte-Uribe, B.; Pérez-Rentero, S.; Lukas, R.; Aviñó, A.; Reina, J. J.; Alkorta, I.; Eritja, R.; Morales, J. C. *Bioconjugate Chem.* **2010**, *21*, 1280.
23. Karskela, M.; Helkearo, M.; Virta, P.; Lönnberg, H. *Bioconjugate Chem.* **2010**, *21*, 748.
24. Kiviniemi, A.; Virta, P.; Lönnberg, H. *Bioconjugate Chem.* **2010**, *21*, 1890.
25. Pourceau, G.; Meyer, A.; Chevolot, Y.; Souteyrand, E.; Vasseur, J.-J.; Morvan, F. *Bioconjugate Chem.* **2010**, *21*, 1520.
26. Jayaprakash, K. N.; Peng, C. G.; Butler, D.; Varghese, J. P.; Maier, M. A.; Rajeev, K. G.; Manoharan, M. *Org. Lett.* **2010**, *12*, 5410.
27. Pourceau, G.; Meyer, A.; Vasseur, J.-J.; Morvan, F. *J. Org. Chem.* **2009**, *74*, 1218.
28. Singh, Y.; Murat, P.; Defrancq, E. *Chem. Soc. Rev.* **2010**, *39*, 2054.
29. Lönnberg, H. *Bioconjugate Chem.* **2009**, *20*, 1065.
30. Karskela, M.; Virta, P.; Malinen, M.; Urtti, A.; Lönnberg, H. *Bioconjugate Chem.* **2008**, *19*, 2549.
31. Kiviniemi, A.; Virta, P.; Lönnberg, H. *Bioconjugate Chem.* **2008**, *19*, 1726.
32. Morvan, F.; Meyer, A.; Jochum, A.; Sabin, C.; Chevolot, Y.; Imberty, A.; Praly, J.-P.; Vasseur, J.-J.; Souteyrland, E.; Vidal, S. *Bioconjugate Chem.* **2007**, *18*, 1637.
33. Duff, R. J.; Deamond, S. F.; Roby, C.; Zhou, Y.; Ts'o, P. O. P. *Methods Enzymol.* **1999**, *313*, 297.
34. Biessen, E. A. L.; Vietsch, H.; Rump, E. T.; Fluiter, K.; Bijsterbosch, M. K.; van Berkel, T. J. C. *Methods Enzymol.* **2000**, *314*, 324.
35. Biessen, E. A. L.; Vietsch, H.; Rump, E. T.; Fluiter, K.; Kuiper, J.; Bijsterbosch, M. K.; van Berkel, T. J. C. *Biochem. J.* **1999**, *340*, 783.
36. Zhu, L.; Ye, Z.; Chemg, K.; Miller, D. D.; Mahato, R. I. *Bioconjugate Chem.* **2008**, *19*, 290.
37. Hamzavi, R.; Dolle, F.; Tavitian, B.; Dahl, O.; Nielsen, P. E. *Bioconjugate Chem.* **2003**, *14*, 941.
38. Biessen, E. A. L.; Sliedregt-Bol, K.; Hoen, P. A. Chr. T.; Prince, P.; Van der Bilt, E.; Valentijn, A. R. P. M.; Meeuwenoord, N. J.; Princen, H.; Bijsterbosch, M. K.; Van der Marel, G. A.; Van Boom, J. H.; Van Berkel, T. J. C. *Bioconjugate Chem.* **2002**, *13*, 295.

39. Rajeev, K. G.; Zimmermann, T.; Manoharan, M.; Maier, M.; Kuchimanchi, S.; Charisse, K. Patent WO 2013075035 A1, **2013**.
40. Prakash, T. P.; Graham, M. J.; Yu, J.; Carty, R.; Low, A.; Chappell, A.; Schmidt, K.; Zhao, C.; Aghajan, M.; Murray, H. F.; Riney, S.; Booten, S. L.; Murray, S. F.; Gaus, H.; Crosby, J.; Lima, W. F.; Guo, S.; Monia, B. P.; Swayze, E. E.; Seth, P. P. *Nucleic Acids Res.* **2014**, *42*, 8796.
41. An, F.; Gong, B.; Wang, H.; Yu, D.; Zhao, G.; Lin, L.; Tang, W.; Yu, H.; Bao, S.; Xie, Q. *Apoptosis* **2012**, *17*, 702.
42. Guo, C. J.; Pan, Q.; Li, D. G.; Sun, H.; Liu, B. W. *J. Hepatol.* **2009**, *50*, 766.
43. Liu, W.; Hao, G.; Long, M. A.; Anthony, T.; Hsieh, J.-T.; Sun, X. *Angew. Chem., Int. Ed.* **2009**, *48*, 7346.
44. Lendvai, G.; Velikyan, I.; Bergström, M.; Estrada, S.; Laryea, D.; Välilä, M.; Salomäki, S.; Långström, B.; Roivainen, A. *Eur. J. Pharm. Sci.* **2005**, *26*, 26.
45. Roivainen, A.; Tolvanen, T.; Salomäki, S.; Lendvai, G.; Velikyan, I.; Numminen, P.; Välilä, M.; Sipilä, H.; Bergström, M.; Härkönen, P.; Lönnberg, H.; Långström, B. *J. Nucl. Med.* **2004**, *45*, 347.
46. Schlesinger, J.; Koezle, I.; Bergmann, R.; Tamburini, S.; Bolzati, C.; Tisato, F.; Noll, B.; Klussmann, S.; Vonhoff, S.; Wuest, F.; Pietzsch, H.-J.; Steinbach, J. *Bioconjugate Chem.* **2008**, *19*, 928.
47. Li, Y.; Schaffer, P.; Perrin, D. M. *Bioorg. Med. Chem. Lett.* **2013**, *23*, 6313.
48. Rockey, W. M.; Huang, L.; Kloepping, K. C.; Baumhover, N. J.; Giangrande, P. H.; Schultz, M. K. *Bioorg. Med. Chem.* **2011**, *19*, 4080.
49. Kiviniemi, A.; Mäkelä, J.; Mäkilä, J.; Saanijoki, T.; Liljenbäck, H.; Poijärvi-Virta, P.; Lönnberg, H.; Laitala-Leinonen, T.; Roivainen, A.; Virta, P. *Bioconjugate Chem.* **2012**, *23*, 1981.
50. Katajisto, J.; Virta, P.; Lönnberg, H. *Bioconjugate Chem.* **2004**, *15*, 890.
51. Salo, H.; Virta, P.; Hakala, H.; Prakash, T. P.; Kawasaki, A. M.; Manoharan, M.; Lönnberg, H. *Bioconjugate Chem.* **1999**, *10*, 815.
52. Brask, J.; Jensen, K. *Bioorg. Med. Chem. Lett.* **2001**, *11*, 697.
53. Joosten, J. A. F.; Loimaranta, V.; Appeldoorn, C. C. M.; Haataja, S.; El Maate, F. A.; Liskamp, R. M.; Finne, J.; Pieters, R. J. *J. Med. Chem.* **2004**, *47*, 6499.
54. Lee, Y. C. *FASEB J.* **1992**, *6*, 3193.